Differential gene expression and chromatin accessibility in the rat medial prefrontal cortex mediating individual variability in vulnerability to opioid use

Shirelle X. Liu[1,2], Peter Muelken[4], Zia L. Maxim[1], Aarthi Ramakrishnan[5], Molly S. Estill[5], Mark G. LeSage[1,3,4], John R. Smethells[3,4], Li Shen[5], Phu V. Tran[2], Andrew C. Harris[1,3,4], and Jonathan C. Gewirtz[1,6]

[1]Department of Psychology, [2]Pediatrics, and [3]Medicine, University of Minnesota; [4]Hennepin Healthcare Research Institute; [5]Icahn School of Medicine at Mount Sinai; [6]Arizona State University

Abstract: Opioid use disorder (OUD) is a neuropsychological disease that causes immense distress to individuals and the society. Despite the abundant clinical and preclinical studies demonstrating substantial individual differences in OUD vulnerability, the neurobiological mechanisms underlying such individual variability in OUD vulnerability remain unclear, hindering the progress in the development of more effective therapeutics. To address this question, we investigated the transcriptome (RNA-seq) and genome-wide chromatin accessibility (ATAC-seq) in the medial prefrontal cortex (mPFC) of male and female rats given morphine and exhibiting differential vulnerability to OUD as measured in behavioral paradigms capturing different phases of the disorder: Withdrawal-Induced Anhedonia (WIA), Demand, and Reinstatement. Ingenuity Pathway Analysis (IPA) of RNA-seq revealed greater changes in canonical pathways in Resilient (vs. Saline) rats in comparison to Vulnerable (vs. Saline) rats across 3 paradigms, suggesting brain adaptations that might contribute to resilience to OUD. Weighted Gene Co-Expression Network Analysis and IPA analyses suggested an involvement of myelination and oligodendrocyte processes, and neuroinflammation responses in the vulnerability associated with WIA and Demand paradigm, respectively. HOMER motif analysis of ATAC-seq showed changes in accessibility to a small set of transcription factor (TF) binding sites, some that were shared across the 3 paradigms and others that were unique to each. In conclusion, we have identified changes in biological pathways, TFs, and their binding motifs that vary with paradigm and disease vulnerability. These findings point to the involvement of distinct transcriptional and epigenetic mechanisms in response to opioid exposure, vulnerability to OUD, and different stages of the disorder.

1. Introduction

Opioid use disorder (OUD) is a neuropsychological disease with profound effects on the individual and the society in which they live. Beyond its multiple social, psychological, behavioral, and economic impacts, OUD is responsible for the large majority of drug overdose deaths in the US and elsewhere (refs). While OUD is a chronic and relapsing disease, with low rates of long-term recovery, changes in synaptic and cellular function have demonstrated in various animal models from the earliest episodes of drug exposure. However, it is unclear the extent to which mechanisms of plasticity that underly the incipient phase of addiction also underly later phases of OUD involving persistent and compulsive drug use and relapse after a period of abstinence.

Given the persistent and relapsing nature of the disorder, such mechanisms presumably involve stable, epigenetic changes in gene regulation that affect long-term behavioral outcomes (Gibney & Nolan, 2010; Werner, Altshuler, Shaham, & Li, 2021). A recent study found changes in gene transcription related to a range of functions including extra-cellular matrix formation and inflammation in multiple brain regions

shortly after heroin self-administration in mice and after later relapse (Browne et al., 2023). Several studies have also looked at changes in gene expression after initial opioid exposure (S. X. Liu et al., 2021; Spijker et al., 2004). The advantage of such noncontingent drug administration paradigms is that drug dosage is fixed and equated across subjects. On the other hand, many of the transcriptional changes seen may be related to effects of opioids that are not related to their addictive potency. Nevertheless, we have found that one measure of repeated, acute morphine exposure – withdrawal-induced anhedonia (WIA), indexed as an increase in thresholds for intracranial self-stimulation (ICSS) – predicts the strength of a variety of measures of subsequent morphine self-administration (MSA). This behavioral phenotype may therefore be useful for homing in on epigenetic changes that are relevant to later drug-taking, as well as for identifying changes associated with individual differences in vulnerability to addiction.

The goal of the present study was to identify alterations in gene regulation across the trajectory of OUD, modeled behaviorally in Sprague-Dawley rats. WIA was used to capture the incipient phase of opioid exposure. To index the severity of chronic opioid-seeking once acquired, we used the behavioral economic measure of Demand, which reflects the degree effort the individual will apply to receive reinforcement. This measure has been validated across species, including in many human studies of addiction (Bentzley, Fender, & Aston-Jones, 2013; Bickel, Johnson, Koffarnus, MacKillop, & Murphy, 2014). Finally, to measure relapse, we used a cue/drug-induced reinstatement paradigm, the neurobiological substrates of which have been extensively investigated (Fredriksson et al., 2021).

For each of the paradigms, we used RNA-seq to assay differential gene transcription across the genome and ATAC-seq to assay chromatin accessibility to transcription factors (TFs), which directly affects levels of gene expression (Klemm, Shipony, & Greenleaf, 2019). These assays were conducted on the medial prefrontal cortex (mPFC), which forms a critical nexus in reinforcement learning circuitry. When it came to both differential TF binding and gene expression, some effects were specific to a particular phase of OUD, whereas others spanned multiple phases. Somewhat surprisingly, we found that changes in canonical pathways were more pronounced across all three paradigms in resilient rats compared to vulnerable rats. Finally, some of the changes we saw were consistent with findings using other approaches, thereby supporting the validity of or approach, whereas others were novel. Among the latter, we found that early opioid exposure reduced co-expression of afunctional network of genes involved in oligodendrocyte maturation/myelination, consistent with evidence of reduced white matter volume in various forms of drug addiction. Overall, our findings provide new directions for the discovery of potential treatments for OUD.

2. Materials and Methods

2.1. Animals

Experimentally-naïve male and female adult Sprague Dawley rats (Inotiv, Lafayette, IN) weighing 276-300 g (male) or 225-250 g (female) at arrival were used. All rats were individually housed in a temperature- and humidity-controlled colony room with unlimited access to water under a reversed 12-h light/dark cycle. All behavioral testing occurred during the dark (active) phase. Beginning one week following arrival, food was restricted to 18 g/day to facilitate operant performance, avoid detrimental health effects of long-term *ad libitum* feeding, and limit catheter migration in rats tested for MSA. All procedures were approved by the Institutional Animal Care and Use Committee (IACUC) of the Hennepin Health Research Institute and University of Minnesota in accordance with the NIH Guide for the Care and

Use of Laboratory Animals and the Guidelines for the Care and Use of Mammals in Neuroscience and Behavioral Research.

2.1.1. Behavioral experiments

Experiment 1: Withdrawal-induced anhedonia

Rats were prepared and trained on a discrete-trial ICSS procedure (see Supplemental Material) in daily ≈ 1 hour sessions conducted Mon-Fri until ICSS thresholds were stable (<10% variability over 5 days). On the first test day, rats were tested for ICSS and then immediately injected with either 5.6 mg/kg morphine sulfate (n = 26, 16 males and 10 females) or saline (n = 13, 8 males, 5 females). ICSS was then tested 23 hours later to measure spontaneous withdrawal, which was expected at this timepoint (Holtz, Radke, Zlebnik, Harris, & Carroll, 2015; J. Liu & Schulteis, 2004; Swain et al., 2020). All rats were then injected as on the preceding day. This injection regimen was repeated for 11 days, with ICSS tested 23 hours after each injection except for a 2-day weekend break in behavioral testing following the 5th and 6th injections. On these days, injections were administered at their usual time. Immediately after the final ICSS test (24 hours after the final morphine or saline injection), rats were sacrificed and tissue from multiple brain structures was harvested and preserved. This is a standard time point for evaluating effects of drugs or other manipulations on the transcriptome and epigenome (Feng et al., 2014; Hodes et al., 2015; M. Li et al., 2017; Walker et al., 2018). The morphine group was larger than the saline group to allow stratification into high and low WIA groups (see below).

Experiment 2: Demand

Rats were implanted with i.v. catheters and allowed to respond for i.v. infusions of 0.4 mg/kg morphine (n = 23, 11 males, 12 females) or saline (n = 11, 5 males, 6 females) during daily 2-hr sessions conducted 7 days per week using our standard apparatus and procedures (see Supplementary Material). Rats were tested under a fixed ratio (FR) 1 schedule for at least 10 sessions and until robust responding was observed, at which point the FR response requirement was increased to FR 2 for at least 5 sessions. The FR was then increased to FR 3 for at least 10 sessions and until acquisition criteria were met (⩾10 infusions per session, ⩽20% coefficient of variation, and ⩾2:1 response ratio on the active versus inactive lever across 3 sessions). To test demand, the FR requirement was increased each day as follows: FR 1, 2, 3, 6, 12, 24, 48, 96. Morphine consumption under this protocol is well described by the current exponential demand function (Swain, Muelken, LeSage, Gewirtz, & Harris, 2018; Swain et al., 2020). Twenty-four hours after completion of demand testing, brains were harvested as described in Experiment 1. Rats in the saline group did not acquire stable SA under the FR 3 schedule and therefore were not tested for demand. Brain collection in these animals occurred on the same day as that for a control-paired morphine rat that began the protocol at a similar time.

Experiment 3: Reinstatement

Male and female rats (n = 26, 12 males, 14 females) were implanted with i.v. catheters and allowed to respond for infusions of 0.4 mg/kg/infusion under an FR 1 schedule as described in Experiment 2. Following at least 10 sessions and attainment of stable responding (same stability criteria as described for Experiment 2), extinction conditions were introduced in which active lever responses resulted in saline infusions in the absence of the drug-associated cue light. Extinction was tested for a minimum of 21 sessions and until responding decreased by 75%, or 42 days of extinction, whichever occurred first, prior to reinstatement testing. During an initial “baseline” session, rats were given a s.c. saline injection 10 minutes prior to the session, and active lever responses continued to deliver saline infusions in the absence of the drug-associated cue light. To test morphine + cue-induced reinstatement, the following

day rats were injected s.c. with morphine (1.0 mg/kg) 10 min prior to the session. Active lever presses during that session resulted in saline infusions and the presentation of the drug-associated cue light. Brain samples were collected 24 hours later. This morphine dose has been shown to reliably elicit reinstatement (Swain et al., 2020). Reinstatement was induced by combined exposure to morphine + cue because this condition produces more robust reinstatement than either morphine or the cue alone (Swain et al., 2020). A negative control group (n = 13, 6 males, 7 females) was allowed to respond for i.v. infusions of saline throughout the protocol. To control for the visual stimulus conditions of the morphine group, control rats had saline delivered in the presence of the cue light for the same number of "acquisition" sessions as a control-paired morphine rat. Likewise, the same number of "extinction" sessions were conducted as the control-paired morphine rate and thus, no cue light was produced with saline deliveries. During "reinstatement", the negative control rats were administered s.c. saline 10 min prior to both test sessions, wherein active lever presses had no consequences during the first "baseline" session but would produce the saline-associated cue during the second "reinstatement" test session. Brain samples in these rats were collected 24 hours after the "reinstatement" assessment.

2.1.2. Statistical analysis

Withdrawal-induced anhedonia. ICSS thresholds and response latencies served as the measure of brain reinforcement function and general motoric function, respectively. Baseline ICSS thresholds (in µA) and response latencies (in sec) were defined as the mean during the last five sessions prior to withdrawal testing. These data were analyzed using separate 2-factor ANOVAs with morphine dose (0 or 5.6 mg/kg) and sex as between-subject factors. ICSS thresholds and latencies during withdrawal testing were subsequently expressed as a percentage of baseline and analyzed using a 3-factor ANOVA with morphine dose and sex as between-subject factors and session as a within-subject factor. Rats were assigned to High and Low WIA groups based on a median split of average ICSS thresholds (% baseline) across all test sessions.

Demand. Infusions per day during the last 5 sessions of acquisition were compared using 3-factor ANOVA with morphine unit dose (0 or 0.4 mg/kg/infusion) and sex as between-subject factors and session as a within-subject factor. Infusions at each FR during demand testing in the morphine group were compared using a one-factor ANOVA with the FR requirement as a within-subject factor, followed by Dunnett's post hoc tests comparing infusions at FR 1 to those at subsequent FRs. To measure demand, exponential demand curve analyses were conducted as described in the Supplementary Material. The derived parameter α measures the degree to which a drug maintains SA following increases in unit price (FR / unit dose), and serves as an index of opioid reinforcement efficacy. Assignment to High and Low demand groups was based on a median split of α values.

Reinstatement. Active and inactive lever responses during saline and morphine-primed reinstatement testing were examined in males and females using a 3-factor (Sex x Reinstatement Drug x Lever type) ANOVA, further analysis with sex collapsed were conducted using a 2-factor ANOVA and a Šidák post-hoc test to determine within-factor differences. Assignment to High and Low reinstatement groups was based on a median split of reinstatement scores, defined using the formula: (active - inactive responses during reinstatement test) - (average of last 3 days of active - inactive responses during extinction).

2.2. mPFC dissection

Rats were deep anesthetized with isoflurane before decapitation. Brains were removed and dissected on an ice-cold metal block. The mPFC from both hemispheres was isolated and aliquoted, flash-frozen in liquid nitrogen, and stored at -80°C.

2.3. RNA isolation and DNA transposition

Total RNA was isolated using the RNAqueous™-Micro Kit (Invitrogen) according to the manufacturer's protocol. Nuclei isolation and DNA transposition were carried out as previously described (Corces et al., 2017) with modifications. Briefly, flash-frozen mPFC was thawed in cold homogenization buffer (5 mM $CaCl_2$, 3 mM $Mg(AC)_2$, 10 mM Tris pH 7.8, 0.0167 mM PMSF, 0.167 mM β-mercaptoethanol, 1x proteinase inhibitor (cOmplete), 320 mM sucrose, 0.1 mM EDTA, 0.1% CA630), and homogenized using a Pellet Pestle motor and syringe. Equal volume of 50% iodixanol solution (5 mM $CaCl_2$, 3 mM $Mg(AC)_2$, 10 mM Tris pH 7.8, 0.017 mM PMSF, 0.17 mM β-mercaptoethanol, 1x proteinase inhibitor (cOmplete), 50% iodixanol) was added to homogenate to reach a final concentration of 25% iodixanol. 30% (5 mM $CaCl_2$, 3 mM $Mg(AC)_2$, 10 mM Tris pH 7.8, 0.017 mM PMSF, 0.17 mM β-mercaptoethanol, 1x proteinase inhibitor (cOmplete), 160 mM sucrose, 30% iodixanol) and 40% (5 mM $CaCl_2$, 3 mM $Mg(AC)_2$, 10 mM Tris pH 7.8, 0.017 mM PMSF, 0.17 mM β-mercaptoethanol, 1x proteinase inhibitor (cOmplete), 160 mM sucrose, 40% iodixanol) iodixanol solution were sequentially added under the 25% iodixanol solution layer. The 3-layer system was centrifuged in a swinging bucket centrifuge at 4255 x g for 30 min. After centrifugation, nuclei were isolated and collected from the 30%-40% iodixanol solution interface. Isolated nuclei were counted with trypan blue (0.4%) and 50,000 nuclei were transferred into a tube containing 1 ml ATAC-RSB (10 mM Tris pH 7.8, 10 mM NaCl, 3 mM $MgCl_2$) with 0.1% Tween-20. Nuclei were pelleted by centrifugation at 500 x g for 10 min. All steps above were conducted on ice or at 4°C. Nuclei were resuspended in transposition mix (25 µL 2x TD buffer (Illumina), 16.5 µL PBS, 0.5 µL 10% Tween-20, 1% digitonin, 2.5 µL Tn5 transposase (Illumina), 5 µL H_2O), and incubated at 37°C for 30 min in a thermomixer at 1000 rpm. Transposed DNA was purified using MinElute Reaction Cleanup kit (Qiagen).

2.4. Library preparation and sequencing

Isolated RNA and DNA were submitted to the University of Minnesota Genomics Center for quality control, library preparation and sequencing. For RNA-seq, total RNA was quantified using the RiboGreen RNA Assay kit (Invitrogen) and assessed for quality using capillary electrophoresis (Agilent BioAnalyzer 2100; Agilent). Barcoded libraries were constructed for each sample using the TruSeq RNA v2 kit (Illumina). For ATAC-seq, DNA was first quantified using the PicoGreen dsDNA Assay Kit (Invitrogen). ATAC-seq library preparation was performed in accordance with the ATAC-seq protocol as described by Buenrostro et al. (2015). Libraries were assessed for quality using capillary electrophoresis (Agilent BioAnalyzer 2100; Agilent). RNA-seq and ATAC-seq libraries were size-selected for ~200 and 200~800 bp fragments, respectively. Selected libraries were sequenced at a depth of ~100 million reads per sample using NovaSeq 6000.

2.5. RNA- and ATAC-seq analysis

Raw sequencing reads were aligned to the Ensembl v90 rat reference genome (rn6) using HISAT2 (v2.2.1) (Kim, Paggi, Park, Bennett, & Salzberg, 2019). Differential gene expression analysis was performed in R (v4.0.2) using the DESeq2 package (Love, Huber, & Anders, 2014). MACS (v2.1.0) was utilized to assess sites (peaks) of chromatin accessibility in ATAC-seq samples (Y. Zhang et al., 2008). MACS2 was run with parameters -p 1e-05 --nomodel --shift 100 --extsize 200. diffReps (Shen et al., 2013) was utilized with default parameters to find differential sites between the comparison groups. Differential sites were mapped to genes using the tool HOMER (PMID: 20513432) (Heinz et al., 2010). Significance was set at absolute log2(Fold Change) > 0.32 and $p < 0.05$ for RNA-seq, $q < 0.05$ for ATAC-seq.

2.6. Weighted gene coexpression network analysis (WGCNA)

WGCNA was used to identify genes that were coexpressed in morphine animals from each paradigm. Gene expression data were analyzed using the WGCNA package in R (Langfelder & Horvath, 2008). Each module was named with an arbitrary color. Differential Gene Correlation Analysis (DGCA) was employed

to quantify differential connectivity between morphine and saline animals. A positive mean differential connectivity (MeDC) score suggests gained connectivity, and a negative MeDC score indicates loss of connectivity. Significance was set at $p < 0.05$.

2.7. Ingenuity Pathway Analysis (IPA)

Differentially expressed genes (DEGs) were annotated by Ingenuity pathway Analysis (IPA; Qiagen) to identify relevant canonical pathways, molecular networks and cellular functions that showed significant alterations between comparison groups as previously described (Barks, Fretham, Georgieff, & Tran, 2018). Statistical significance ($p < 0.05$; -log(p) > 1.3) was determined by Fisher's exact test.

2.8. HOMER motif analysis

The program 'findMotifsGenome.pl' from the tool HOMER (PMID: 20513432) (Heinz et al., 2010) was utilized to identify motifs of transcription factors among differential sites identified by diffReps (PMID: 23762400) (Shen et al., 2013) after applying an absolute log2(Fold Change) cutoff of 0.32 and a q-value cutoff of 0.05.

3. Results

3.1. Rats showed individual differences in behaviors reflecting OUD vulnerability

3.1.1. Experiment 1: Withdrawal-induced anhedonia

Baseline ICSS thresholds and response latencies did not differ between groups (data not shown). A 3-way ANOVA on ICSS thresholds during withdrawal testing indicated a significant main effect of morphine dose (F (1, 35) = 20.3, $p < 0.0001$), reflecting an elevation in ICSS thresholds in morphine-treated compared to saline-treated rats (Figure 1A), but no significant effects of sex, session, or interactions between these variables. ICSS response latencies were not significantly affected during withdrawal (data not shown), indicating that the ICSS threshold data were not influenced by non-specific (e.g., motoric) effects.

3.1.2. Experiment 2: Demand

Rats reliably acquired morphine SA, with infusions per day significantly higher in the morphine SA versus saline SA group for both sexes at the end of the acquisition period (data not shown). Analysis of infusions during FR escalation indicated a significant effect of FR value, (F (1.6, 32.3) = 29.4, $p < 0.0001$), but no effect of sex or FR x sex interaction. Comparison of data collapsed across sex indicated that infusions were decreased compared to FR 1 at all FR values $\geqslant$ FR 3 (Dunnett q = 2.9 - 6.3, $p < 0.05$ or 0.01; Figure 1B). Morphine consumption during demand testing was well described by an exponential demand function, with R^2 values typically $\geqslant$ 0.85 for individual animals (data not shown) and R^2 = 0.99 for rats as a group (Figure 1C).

3.1.3. Experiment 3: Reinstatement

A 3-factor ANOVA indicated no main effect or interactions related to sex, but there was a main effect of lever type (active vs. inactive; F(1, 24) = 26.73, $p < 0.0001$), reinstatement condition (Saline + No cue vs. Morphine + Cue; F(1, 24) = 22.22, $p < 0.0001$), and an interaction between these two factors (F(1, 24) = 23.59, $p < 0.0001$). A follow-up 2-factor ANOVA on the data collapsed across sexes found a significant interaction of reinstatement condition and lever type (F(1, 50) = 20.63, $p < 0.0001$)) with a Šidák post-hoc comparison revealing significantly greater responding on only the active lever (t_{24} = 6.855) following

Morphine + Cue exposure vs. Saline + No Cue exposure (Figure 1D). In the saline control group a 3-factor ANOVA revealed a main effect of lever type ($F(1, 11) = 54.00$, $p < 0.0001$), but no main effect or interaction with sex. After collapsing across sex, a 2-factor ANOVA a main effect of lever type was observed ($F(1, 24) = 46.76$, $p < 0.0001$) and a lever type x reinstatement condition (no cue vs. cue) ($F(1, 24) = 6.47$, $p < 0.05$), with a Šidák post-hoc comparison revealing significantly lower active-lever responding ($t_{24} = 3.123$) following Sal + Cue exposure vs. Saline + No Cue exposure (data not shown).

Our behavioral data showed a considerable degree of individual variability for all three measures (see z-score distribution in Figure 1E).

3.2. Differences in canonical pathways altered in resilient versus vulnerable male rats

Principal component analysis (PCA) plots of RNA-seq data revealed 15%-23% variations in the top 500 expressed genes among male and female transcriptomes were explained by drug treatment, whereas 17%-25% of the variations were explained by sex (Supplemental figure 1). Due to such strong sex effects, NGS data were analyzed in a sex-separated manner. Numbers of DEGs in each comparison pair were summarized in Table 1 and 2. Contrary to our expectations, IPA canonical pathway analysis of these DEGs suggested that a greater number of biological pathways were altered in resilient compared to vulnerable male rats across all three paradigms (Figure 2). Similar trends were also found in female WIA and Reinstatement paradigms, but not in the Demand paradigm (Supplemental figure 2). Altered canonical pathways were associated with signaling pathways in the nervous system (e.g., CREB, LTP, LTD, Opioid signaling), inflammation (e.g., Neuroinflammation, IL-4, IL-10, S100 family), and metabolism (e.g., Oxidative phosphorylation).

3.3. Myelination-related gene networks were implicated in OUD vulnerability with sex-specific patterns

Differential connectivity of genes in WGCNA modules between morphine and saline animals was detected in 5 modules built with male and female morphine WIA rats (Figure 3A). Gene Ontology (GO) analysis revealed a “saddlebrown” module specifically involved in oligodendrocyte functions and myelination that showed decreased connectivity in morphine rats (Figure 3B). A similar myelination/oligodendrocyte module with differential connectivity between morphine and saline animals was also identified in WGCNA networks built with morphine and saline Demand rats in both sexes (Supplemental figure 3). IPA upstream regulator analysis predicted changes in activities of 2 TFs that function in myelination, TCF7L2 and SOX2, in WIA animals in both sexes (Figure 4, male; Figure 5, female). Interestingly, these TFs were predicted to be more significantly inhibited in the resilient group in males, yet more significantly activated in the vulnerable group in females (Figure 4, male; Figure 5, female). This contrast indicated the same biological mechanism underlying OUD vulnerability can be carried out by drastically different gene networks between sexes (Figure 6).

3.4. Neuroinflammatory responses were dependent on the stages and resiliency in OUD

Differential connectivity of genes in WGCNA modules between morphine and saline animals was detected in 6 modules built with male and female morphine Demand rats (Figure 7A). GO analysis revealed “white” module which showed decreased connectivity in morphine rats highly specifically involved in immune response/inflammation (Figure 7B). IPA canonical pathway analysis of male and female Demand RNA-seq data corroborated such observation (Figure 8). Strikingly, further examinations revealed that resilient male rats showed an activation in inflammation-related pathways, whereas vulnerable rats showed a moderate inhibition in the same pathways (Figure 8A). In female animals, inflammation pathways in resilient individuals remained largely unchanged, and were inhibited in vulnerable individuals (Figure 8B).

Aside from the sex and resiliency, changes in inflammation pathways also varied with paradigms. Both male and female resilient rats exhibited strong inhibition of inflammation pathways in the WIA paradigm, but activation (male) or reduced inhibition (female) of the same pathways in the Demand and Reinstatement paradigms (Figures 9 and 10). Vulnerable rats in general showed inhibition of these pathways in both male and female rats across 3 paradigms (Figures 9 and 10).

3.5. Morphine exposure dysregulated metabolic processes

Differential connectivity of genes in WGCNA modules between morphine and saline animals was detected in 6 modules built with male and female morphine Reinstatement rats (Figure 11A). GO analysis revealed “darkgreen” module which showed decreased connectivity in morphine rats highly specifically involved in metabolic processes (Figure 11B). This observation was also supported by connectivity change in the “lightcyan1” module built with morphine and saline Reinstatement rats (Supplemental figure 4).

3.6. Chromatin accessibility of top transcription factor binding sites showed paradigm specificity

HOMER motif analysis revealed TFs associated with these sites. Among the top 10 significant TFs in males, members of AP-1 family (e.g., Fos, JunB, Fra, Atf) were found in morphine exposed rats in all three paradigms, but not between resilient verses vulnerable groups (Table 3, Supplemental table xx). In contrast, members of MEF2 (i.e., MEF2a-d) and bHLH (e.g., Atoh1, Npas4) families were also associated with OUD vulnerability (Table 3, Supplemental table xx). Members of NR family (e.g., PGR, GRE) were specific to the Reinstatement paradigm with no significant differences between resilient verses vulnerable groups (Table 3).

4. Discussion

In this study, we evaluated behavioral vulnerability to MSA in male and female rats in 3 paradigms representing different phases along the trajectory of OUD: WIA, Demand, and Reinstatement. We then compared gene transcription and chromatin accessibility across the genome in the mPFC both as a function of drug treatment and individual differences in behavioral outcomes to identify molecular and cellular mechanisms underlying vulnerability to OUD. We discovered key brain processes and epigenetic regulators associated with susceptibility to OUD that are shared and unique to each paradigm, as well as those that differ by sex. These results will provide important insights on the development of more effective and personalized therapeutics for OUD.

Perhaps the most striking and unexpected observation was that gene expression in canonical pathways was more profoundly altered in resilient rats compared to vulnerable rats. We saw this pattern across the three behavioral models in male rats, although it was strongest in the WIA and Reinstatement paradigms. It is commonly believed that the magnitude of dysregulated biological processes upon substance exposure is positively correlated with addiction severity, and that addiction is a result of passive brain maladaptation to the pharmacological effects of addictive substances (Tiwari, Sharma, Pandey, & Shukla, 2020; Wise & Robble, 2020). However, recent studies have also raised the possibility that resilience to substance use disorders might be mediated by mechanisms that are distinct from those contributing to addiction susceptibility (Ersche et al., 2020; Miela, Cubała, Mazurkiewicz, & Jakuszkowiak-Wojten, 2018). Our results, especially in the WIA and the Reinstatement models in both males and females, strongly supported this emerging perspective of OUD vulnerability; namely, that vulnerability to OUD could be the consequence of inadequate compensatory adaptations to the drug as much as, or more than, a consequence of excessive maladaptive responses to the drug. Given evidence that there are distinctive waves of gene expression across the passage of time during abstinence, including changes in the directionality of gene expression (Browne et al., 2023; Spijker et al., 2004), it is

possible that the relationship between the degree of gene expression in functional pathways and vulnerability would be reversed either in the immediate aftermath of morphine exposure, and/or after longer term abstinence. In either case, our findings highlight the importance of accounting for individual differences in addiction vulnerability at both behavioral and mechanistic levels, and of entertaining the possibility that resilience to OUD is associated with enhanced transcription in addiction-associated functional pathways.

Among gene modules that appear to exhibit inadequate recruitment in vulnerable rats, the most notable to emerge was a network associated with myelination and oligodendrocyte maturation in the WIA paradigm. Specifically, WGCNA revealed reduced connectivity in this network upon morphine treatment. GO analysis indicated relevant functionality in >20% of the genes in this network. One of these, the TF-coding *Prdm8*, which was revealed through ARACNe as having substantial regulatory connections with other genes in the network, is a member of the PRDM TF family that broadly regulate gene activity through chromatin regulation and are themselves regulated through DNA methylation (Di Tullio, Schwarz, Zorgati, Mzoughi, & Guccione, 2022). PRDM8 in particular is involved in repressing the production of oligodendrocyte precursor cells (Scott, O'Rourke, Gillen, & Appel, 2020).

Consistent with these network analysis findings, a comparison of gene expression in behaviorally vulnerable and resilient males in the WIA paradigm revealed two TFs, TCF7L2 and SOX2, as more strongly inhibited in resilient rats. These TFs positively regulate oligodendroglial proliferation and differentiation, as well as CNS myelination and remyelination post injury (Benraiss et al., 2022; Fu, Kesari, & Cai, 2012; S. Zhang et al., 2018). Interestingly, although sharing only 5 DEGs with the males, TCF7L2 and SOX2 networks were also significantly identified in female rats. In addition, in contrast to the strong inhibitory effects in the resilient males, female animals exhibited stronger activation of those networks in the vulnerable group. Taken together, these results suggest a reduced oligodendroglial and myelination process during withdrawal from the initial morphine exposure to be protective against OUD-like behaviors. Supporting the functional relevance of these correlational effects, a recent report indicates that blockade of oligodendrogenesis in the mouse ventrotegmental area (VTA) reduced dopamine release in the nucleus accumbens and induction of a conditioned place preferences for morphine (Yalçın et al., 2022).

While resilience was most closely associated with differential activity in oligodendrogenesis-related pathways in the WIA paradigm, resilience in males in the Demand paradigm was most strongly associated with increased activity in gene pathways associated with neuroimmune function. Furthermore, in a striking parallel to the sex differences we saw in the regulation of oligodendroglial activity, female rats showed the same broad directionality as males, except that greater neuroimmune activities were found in resilient animals. This suggests that proinflammatory responses to opioids (Butelman et al., 2023; Eidson & Murphy, 2019; Seney et al., 2021) may in fact serve a protective function in the domain of opioid addiction liability at the same time that anti-inflammatory responses tend to promote the analgesic effects of opioids (Cuitavi et al., 2023).

While providing a comprehensive snapshot of gene transcription at a given moment in time, the character of the transcriptome can vary greatly across both large (weeks) and small (hours) timescales in response to events such as the circadian cycle and transient environmental fluctuations (J. Z. Li et al., 2013; López-Maury, Marguerat, & Bähler, 2008; Raj & van Oudenaarden, 2008; Sukumaran, Almon, DuBois, & Jusko, 2010). On the other hand, epigenetic modifications that regulate gene expression, either transiently or in a sustained manner, are likely more tightly associated with long-term behavioral outcomes (Gibney & Nolan, 2010). Therefore, we assessed differential chromatin accessibility to TFs in resilient and vulnerable animals across 3 paradigms. AP-1, a TF family that is significantly implicated in

OUD (Browne, Godino, Salery, & Nestler, 2020), was among the top 10 TFs identified by HOMER motif analysis upon morphine exposure (i.e., morphine vs. saline) but was not significantly implicated in resilient vs. vulnerable rats. This suggests that the AP-1 TF family might primarily respond to the pharmacological effects of morphine rather than behavioral vulnerability to OUD. In contrast, chromatin accessibility of the MEF2 and bHLH TF family binding motifs differed significantly in resilient vs. vulnerable rats, suggesting a specific role in OUD vulnerability.

A further distinction between differentially accessible TF motifs was whether they were implicated in one phase of addiction or across all phases. Thus, whereas the AP1 and MEF2 families were implicated across all three paradigms, bHLH was implicated only in Demand and the Nuclear Receptor (NR family, e.g., progesterone receptor, glucocorticoid receptor) in reinstatement. In contrast to the known involvement of AP-1 and MEF2 TF families in addiction-like behavior, the association between bHLH and NR family TFs and opioid addiction vulnerability is novel but coheres with a recent single-nucleus ATAC-seq study implicating both TF families in individual differences in the severity of cocaine self-administration in mice (Zhou et al., 2023).

In summary, we employed 3 behavioral models in rats to capture 3 distinct stages of human OUD: the initial anhedonic response to opioid exposure, economic demand for the drug once drug-taking has been established, and relapse after extinction of drug-taking behavior. Through assays of genomic transcriptional expression and chromatin accessibility, we have identified key biological processes and epigenetic regulators that exhibit shared and unique patterns across rat models of 3 distinct stages of human OUD. The unexpected discovery that more canonical pathways were altered in resilient animals highlights the need of examining the mechanisms underlying phenotypic differences after acute and chronic opioid use. Finally, our findings on the association between susceptibility to OUD and myelination, neuroinflammation, and the bHLH and NR TF families have shed light on potential molecular pathways affecting addiction vulnerability that could serve as candidates for future functional studies.

References

Barks, A., Fretham, S. J. B., Georgieff, M. K., & Tran, P. V. (2018). Early-Life Neuronal-Specific Iron Deficiency Alters the Adult Mouse Hippocampal Transcriptome. *Journal of Nutrition*, *148*(10), 1521–1528. https://doi.org/10.1093/jn/nxy125

Benraiss, A., Mariani, J. N., Tate, A., Madsen, P. M., Clark, K. M., Welle, K. A., … Goldman, S. A. (2022). A TCF7L2-responsive suppression of both homeostatic and compensatory remyelination in Huntington disease mice. *Cell Reports*, *40*(9). https://doi.org/10.1016/J.CELREP.2022.111291

Bentzley, B. S., Fender, K. M., & Aston-Jones, G. (2013). The behavioral economics of drug self-administration: a review and new analytical approach for within-session procedures. *Psychopharmacology*, *226*(1), 113–125. https://doi.org/10.1007/S00213-012-2899-2

Bickel, W. K., Johnson, M. W., Koffarnus, M. N., MacKillop, J., & Murphy, J. G. (2014). The Behavioral Economics of Substance Use Disorders: reinforcement pathologies and their repair. *Annual Review of Clinical Psychology*, *10*, 641. https://doi.org/10.1146/ANNUREV-CLINPSY-032813-153724

Browne, C. J., Futamura, R., Minier-Toribio, A., Hicks, E. M., Ramakrishnan, A., Martínez-Rivera, F. J., … Nestler, E. J. (2023). Transcriptional signatures of heroin intake and relapse throughout the brain reward circuitry in male mice. *Science Advances*, *9*(23). https://doi.org/10.1126/SCIADV.ADG8558

Browne, C. J., Godino, A., Salery, M., & Nestler, E. J. (2020). Epigenetic Mechanisms of Opioid Addiction. *Biological Psychiatry*, *87*(1), 22–33. https://doi.org/10.1016/J.BIOPSYCH.2019.06.027

Buenrostro, J., Wu, B., Chang, H., & Greenleaf, W. (2015). ATAC-seq: A Method for Assaying Chromatin Accessibility Genome-Wide. *Current Protocols in Molecular Biology / Edited by Frederick M. Ausubel ... [et Al.]*, *109*, 21.29.1. https://doi.org/10.1002/0471142727.MB2129S109

Butelman, E. R., Goldstein, R. Z., Nwaneshiudu, C. A., Girdhar, K., Roussos, P., Russo, S. J., & Alia-Klein, N. (2023). Neuroimmune Mechanisms of Opioid Use Disorder and Recovery: Translatability to Human Studies, and Future Research Directions. *Neuroscience*, *528*, 102–116. https://doi.org/10.1016/J.NEUROSCIENCE.2023.07.031

Corces, M. R., Trevino, A. E., Hamilton, E. G., Greenside, P. G., Sinnott-Armstrong, N. A., Vesuna, S., … Chang, H. Y. (2017). An improved ATAC-seq protocol reduces background and enables interrogation of frozen tissues. *Nature Methods 2017 14:10*, *14*(10), 959–962. https://doi.org/10.1038/nmeth.4396

Cuitavi, J., Torres-Pérez, J. V., Lorente, J. D., Campos-Jurado, Y., Andrés-Herrera, P., Polache, A., … Hipólito, L. (2023). Crosstalk between Mu-Opioid receptors and neuroinflammation: Consequences for drug addiction and pain. *Neuroscience & Biobehavioral Reviews*, *145*, 105011. https://doi.org/10.1016/J.NEUBIOREV.2022.105011

Di Tullio, F., Schwarz, M., Zorgati, H., Mzoughi, S., & Guccione, E. (2022). The duality of PRDM proteins: epigenetic and structural perspectives. *The FEBS Journal*, *289*(5), 1256–1275. https://doi.org/10.1111/FEBS.15844

Eidson, L. N., & Murphy, A. Z. (2019). Inflammatory mediators of opioid tolerance: Implications for dependency and addiction. *Peptides*, *115*, 51–58. https://doi.org/10.1016/J.PEPTIDES.2019.01.003

Ersche, K. D., Meng, C., Ziauddeen, H., Stochl, J., Williams, G. B., Bullmore, E. T., & Robbins, T. W. (2020). Brain networks underlying vulnerability and resilience to drug addiction. *Proceedings of the National Academy of Sciences of the United States of America*, *117*(26), 15253–15261. https://doi.org/10.1073/PNAS.2002509117

Feng, J., Wilkinson, M., Liu, X., Purushothaman, I., Ferguson, D., Vialou, V., … Shen, L. (2014). Chronic cocaine-regulated epigenomic changes in mouse nucleus accumbens. *Genome Biology*, *15*(4). https://doi.org/10.1186/gb-2014-15-4-r65

Fredriksson, I., Venniro, M., Reiner, D. J., Chow, J. J., Bossert, J. M., & Shaham, Y. (2021). Animal Models of Drug Relapse and Craving after Voluntary Abstinence: A Review. *Pharmacological Reviews*, *73*(3), 1050–1083. https://doi.org/10.1124/PHARMREV.120.000191

Fu, H., Kesari, S., & Cai, J. (2012). Tcf7l2 is Tightly Controlled During Myelin Formation. *Cellular and Molecular Neurobiology*, *32*(3), 345. https://doi.org/10.1007/S10571-011-9778-Y

Gibney, E. R., & Nolan, C. M. (2010). Epigenetics and gene expression. *Heredity*, *105*(1), 4–13. https://doi.org/10.1038/HDY.2010.54

Heinz, S., Benner, C., Spann, N., Bertolino, E., Lin, Y. C., Laslo, P., … Glass, C. K. (2010). Simple combinations of lineage-determining transcription factors prime cis-regulatory elements required for macrophage and B cell identities. *Molecular Cell*, *38*(4), 576–589. https://doi.org/10.1016/J.MOLCEL.2010.05.004

Hodes, G. E., Pfau, M. L., Purushothaman, I., Ahn, H. F., Golden, S. A., Christoffel, D. J., … Russo, S. J. (2015). Sex Differences in Nucleus Accumbens Transcriptome Profiles Associated with Susceptibility versus Resilience to Subchronic Variable Stress. *Journal of Neuroscience*, *35*(50), 16362–16376. https://doi.org/10.1523/jneurosci.1392-15.2015

Holtz, N. A., Radke, A. K., Zlebnik, N. E., Harris, A. C., & Carroll, M. E. (2015). Intracranial self-stimulation reward thresholds during morphine withdrawal in rats bred for high (HiS) and low (LoS) saccharin intake. *Brain Research*, *1602*(C), 119. https://doi.org/10.1016/J.BRAINRES.2015.01.004

Kim, D., Paggi, J. M., Park, C., Bennett, C., & Salzberg, S. L. (2019). Graph-Based Genome Alignment and Genotyping with HISAT2 andHISAT-genotype. *Nature Biotechnology*, *37*(8), 907. https://doi.org/10.1038/S41587-019-0201-4

Klemm, S. L., Shipony, Z., & Greenleaf, W. J. (2019). Chromatin accessibility and the regulatory epigenome. *Nature Reviews. Genetics*, *20*(4), 207–220. https://doi.org/10.1038/S41576-018-0089-8

Langfelder, P., & Horvath, S. (2008). WGCNA: An R package for weighted correlation network analysis. *BMC Bioinformatics*, *9*(1), 1–13. https://doi.org/10.1186/1471-2105-9-559/FIGURES/4

Li, J. Z., Bunney, B. G., Meng, F., Hagenauer, M. H., Walsh, D. M., Vawter, M. P., … Bunney, W. E. (2013). Circadian patterns of gene expression in the human brain and disruption in major depressive disorder. *Proceedings of the National Academy of Sciences of the United States of America*, *110*(24), 9950–9955. https://doi.org/10.1073/PNAS.1305814110

Li, M., Xu, P., Xu, Y., Teng, H., Tian, W., Du, Q., & Zhao, M. (2017). Dynamic expression changes in the transcriptome of the prefrontal cortex after repeated exposure to cocaine in mice. *Frontiers in Pharmacology*, *8*(MAR), 142. https://doi.org/10.3389/FPHAR.2017.00142/FULL

Liu, J., & Schulteis, G. (2004). Brain reward deficits accompany naloxone-precipitated withdrawal from acute opioid dependence. *Pharmacology, Biochemistry, and Behavior*, *79*(1), 101–108. https://doi.org/10.1016/J.PBB.2004.06.006

Liu, S. X., Gades, M. S., Swain, Y., Ramakrishnan, A., Harris, A. C., Tran, P. V., & Gewirtz, J. C. (2021). Repeated morphine exposure activates synaptogenesis and other neuroplasticity-related gene networks in the dorsomedial prefrontal cortex of male and female rats. *Drug and Alcohol Dependence*, *221*(March 2020), 108598. https://doi.org/10.1016/j.drugalcdep.2021.108598

López-Maury, L., Marguerat, S., & Bähler, J. (2008). Tuning gene expression to changing environments: from rapid responses to evolutionary adaptation. *Nature Reviews. Genetics*, *9*(8), 583–593. https://doi.org/10.1038/NRG2398

Love, M. I., Huber, W., & Anders, S. (2014). Moderated estimation of fold change and dispersion for RNA-seq data with DESeq2. *Genome Biology*, *15*(12). https://doi.org/10.1186/S13059-014-0550-8

Miela, R., Cubała, W. J., Mazurkiewicz, D. W., & Jakuszkowiak-Wojten, K. (2018). The neurobiology of addiction. A vulnerability/resilience perspective. *The European Journal of Psychiatry*, *32*(3), 139–148. https://doi.org/10.1016/J.EJPSY.2018.01.002

Raj, A., & van Oudenaarden, A. (2008). Nature, Nurture, or Chance: Stochastic Gene Expression and Its Consequences. *Cell*, *135*(2), 216–226. https://doi.org/10.1016/J.CELL.2008.09.050

Scott, K., O'Rourke, R., Gillen, A., & Appel, B. (2020). Prdm8 regulates pMN progenitor specification for

motor neuron and oligodendrocyte fates by modulating the Shh signaling response. *Development (Cambridge, England)*, *147*(16). https://doi.org/10.1242/DEV.191023

Seney, M. L., Kim, S. M., Glausier, J. R., Hildebrand, M. A., Xue, X., Zong, W., … Logan, R. W. (2021). Transcriptional Alterations in Dorsolateral Prefrontal Cortex and Nucleus Accumbens Implicate Neuroinflammation and Synaptic Remodeling in Opioid Use Disorder. *Biological Psychiatry*, *90*(8), 550–562. https://doi.org/10.1016/J.BIOPSYCH.2021.06.007

Shen, L., Shao, N.-Y., Liu, X., Maze, I., Feng, J., & Nestler, E. J. (2013). diffReps: Detecting Differential Chromatin Modification Sites from ChIP-seq Data with Biological Replicates. *PLOS ONE*, *8*(6), e65598. https://doi.org/10.1371/JOURNAL.PONE.0065598

Spijker, S., Houtzager, S. W. J., De Gunst, M. C. M., De Boer, W. P. H., Schoffelmeer, A. N. M., & Smit, A. B. (2004). Morphine exposure and abstinence define specific stages of gene expression in the rat nucleus accumbens. *The FASEB Journal : Official Publication of the Federation of American Societies for Experimental Biology*, *18*(7), 848–850. https://doi.org/10.1096/fj.03-0612fje

Sukumaran, S., Almon, R. R., DuBois, D. C., & Jusko, W. J. (2010). Circadian rhythms in gene expression: Relationship to physiology, disease, drug disposition and drug action. *Advanced Drug Delivery Reviews*, *62*(9–10), 904–917. https://doi.org/10.1016/J.ADDR.2010.05.009

Swain, Y., Muelken, P., LeSage, M. G., Gewirtz, J. C., & Harris, A. C. (2018). Locomotor activity does not predict individual differences inmorphine self-administration in rats. *Pharmacology, Biochemistry, and Behavior*, *166*, 48. https://doi.org/10.1016/J.PBB.2018.01.008

Swain, Y., Muelken, P., Skansberg, A., Lanzdorf, D., Haave, Z., LeSage, M. G., … Harris, A. C. (2020). Higher anhedonia during withdrawal from initial opioid exposure is protective against subsequent opioid self-administration in rats. *Psychopharmacology*, *237*(8), 2279. https://doi.org/10.1007/S00213-020-05532-W

Tiwari, R. K., Sharma, V., Pandey, R. K., & Shukla, S. S. (2020). Nicotine Addiction: Neurobiology and Mechanism. *Journal of Pharmacopuncture*, *23*(1), 1. https://doi.org/10.3831/KPI.2020.23.001

Walker, D. M., Cates, H. M., Loh, Y. H. E., Purushothaman, I., Ramakrishnan, A., Cahill, K. M., … Nestler, E. J. (2018). Cocaine Self-administration Alters Transcriptome-wide Responses in the Brain's Reward Circuitry. *Biological Psychiatry*, *84*(12), 867–880. https://doi.org/10.1016/j.biopsych.2018.04.009

Werner, C. T., Altshuler, R. D., Shaham, Y., & Li, X. (2021). Epigenetic mechanisms in drug relapse. *Biological Psychiatry*, *89*(4), 331. https://doi.org/10.1016/J.BIOPSYCH.2020.08.005

Wise, R. A., & Robble, M. A. (2020). Dopamine and Addiction. *Annual Review of Psychology*, *71*, 79–106. https://doi.org/10.1146/ANNUREV-PSYCH-010418-103337

Yalçın, B., Pomrenze, M. B., Malacon, K., Chau, I. J., Taylor, K. R., Ni, L., … Monje, M. (2022). Myelin plasticity in ventral tegmental area is required for opioid reward. *BioRxiv*, 2022.09.01.506263. https://doi.org/10.1101/2022.09.01.506263

Zhang, S., Zhu, X., Gui, X., Croteau, C., Song, L., Xu, J., … Guo, F. (2018). Sox2 Is Essential for Oligodendroglial Proliferation and Differentiation during Postnatal Brain Myelination and CNS Remyelination. *The Journal of Neuroscience*, *38*(7), 1802. https://doi.org/10.1523/JNEUROSCI.1291-17.2018

Zhang, Y., Liu, T., Meyer, C. A., Eeckhoute, J., Johnson, D. S., Bernstein, B. E., … Liu, X. S. (2008). Model-based Analysis of ChIP-Seq (MACS). *Genome Biology 2008 9:9*, *9*(9), 1–9. https://doi.org/10.1186/GB-2008-9-9-R137

Zhou, J. L., de Guglielmo, G., Ho, A. J., Kallupi, M., Pokhrel, N., Li, H. R., … Telese, F. (2023). Single-nucleus genomics in outbred rats with divergent cocaine addiction-like behaviors reveals changes in amygdala GABAergic inhibition. *Nature Neuroscience 2023 26:11*, *26*(11), 1868–1879. https://doi.org/10.1038/s41593-023-01452-y

Figure captions:

Figure 1: (A) ICSS thresholds (% Baseline, Mean ± SEM) during spontaneous morphine withdrawal). *,** Different from Saline (main effect), $p < 0.0001$. (B) Infusions at each FR (Mean ± SEM) during Demand testing. *,** Different from FR 1, $p < 0.05$ or 0.01 (collapsed across sex). (C) Exponential demand function for morphine during demand testing. (D) Active lever presses (Mean ± SEM) during Sal + No Cue or Mor + Cue conditions following extinction of MSA. ** Different from Sal + No Cue, $p < 0.01$. Data are collapsed across sex in Figures 1A – 1D because there were no significant effects of sex in any behavioral model. (E) Z-score distribution for individual rats shown in panels (A)-(D).

Table 1: Numbers of DEGs in each comparison group in males. log2(Fold Change) > 0.32, $p < 0.05$.

Table 2: Numbers of DEGs in each comparison group in females. log2(Fold Change) > 0.32, $p < 0.05$.

Figure 2: Resilient male rats showed greater changes in IPA canonical pathways. (A) Heatmaps of all canonical pathways with detectable alteration in at least one comparison group. Each line represents one pathway. Orange, z-score > 0 ; Blue, z-score<0; White, z-score = 0; Grey, z-score = N/A. (B) Numbers of significantly altered canonical pathways in each comparison group. Absolute z-score ≥ 1, -log(p-value) ≥ 1.3.

Figure 3: WGCNA analyses of WIA male and female animals. (A) 5 modules displayed significant changes in connectivity between morphine vs. saline animals. (B) “saddlebrown” module showed enrichment of genes functioning in oligodendrocyte processes and myelination. (C) ARACNe analyses of genes in the “saddlebrown” module.

Figure 4: IPA upstream regulator analysis predicted the activity of TCF7L2 and SOX2 with more inhibition in resilient WIA male animals.

Figure 5: IPA upstream regulator analysis predicted the activity of TCF7L2 and SOX2 with more activation in vulnerable WIA female animals.

Figure 6: Venn diagram showing 5 overlapping genes between WIA resilient male and vulnerable female TCF7L2 and SOX2 networks.

Figure 7: WGCNA analyses of Demand male and female animals. (A) 6 modules displayed significant changes in connectivity between morphine vs. saline animals. (B) “white” module showed enrichment of genes functioning in immune response/inflammation.

Figure 8: IPA analysis of neuroinflammation-associated pathways in Demand (A) male and (B) female resilient and vulnerable animals. Orange, z-score > 0 ; Blue, z-score<0; White, z-score = 0; dot, absolute z-score < 1.

Figure 9: IPA analysis of top 15 neuroinflammation-associated pathways in male resilient and vulnerable animals in the WIA, Demand, and Reinstatement paradigms. Orange, z-score > 0 ; Blue, z-score<0; White, z-score = 0; dot, absolute z-score < 1.

Figure 10: IPA analysis of top 15 neuroinflammation-associated pathways in female resilient and vulnerable animals in the WIA, Demand, and Reinstatement paradigms. Orange, z-score > 0 ; Blue, z-score<0; White, z-score = 0; dot, absolute z-score < 1.

Figure 11: WGCNA analyses of Reinstatement male and female animals. (A) 6 modules displayed significant changes in connectivity between morphine vs. saline animals. (B) “darkgreen” module showed enrichment of genes functioning in metabolic processes.

Table 3: HOMER motif analysis for male Mor vs. Sal and Resilient (Res) vs. Vulnerable (Vul) ATAC-seq data. Examples of top 10 significantly enriched motifs and their families were shown.

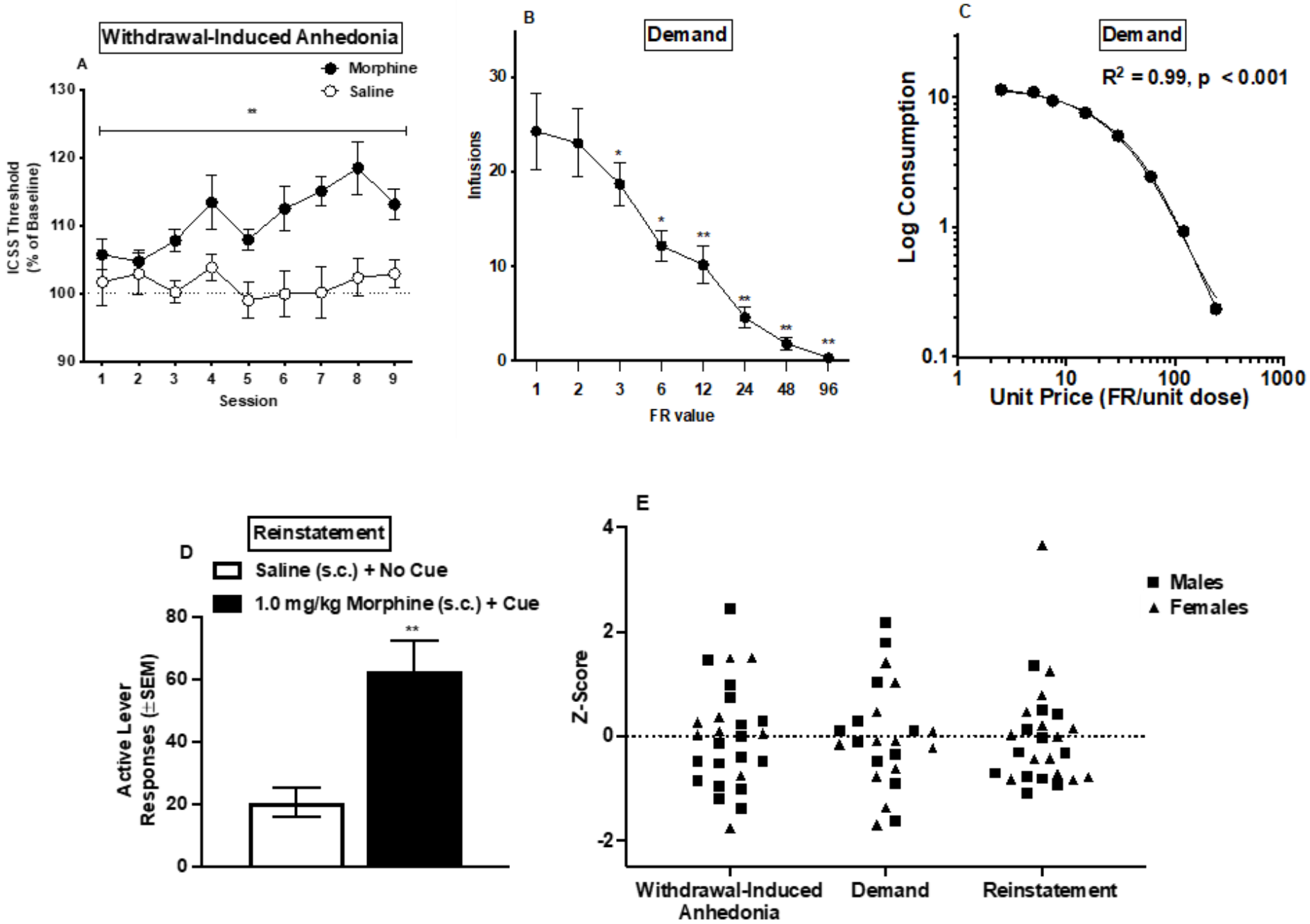
Withdrawal-Induced Anhedonia
A
Morphine
Saline
ICSS Threshold (% of Baseline)
Session
B
Demand
Infusions
FR value
C
Demand
$R^2 = 0.99$, $p < 0.001$
Log Consumption
Unit Price (FR/unit dose)
D
Reinstatement
Saline (s.c.) + No Cue
1.0 mg/kg Morphine (s.c.) + Cue
Active Lever Responses (±SEM)
E
Z-Score
Males
Females
Withdrawal-Induced Anhedonia
Demand
Reinstatement

Paradigm	Group	Total DEGs	Up	Down
WIA	High (Resilient) vs. Sal	1557	804	753
	Low (Vulnerable) vs. Sal	313	147	166
Demand	High α (Resilient) vs. Sal	223	91	132
	Low α (Vulnerable) vs. Sal	472	259	213
Reinstatement	Low (Resilient) vs. Sal	448	227	221
	High (Vulnerable) vs. Sal	488	278	210

Paradigm	Group	Total DEGs	Up	Down
WIA	High (Resilient) vs. Sal	560	125	435
	Low (Vulnerable) vs. Sal	655	199	456
Demand	High α (Resilient) vs. Sal	304	104	200
	Low α (Vulnerable) vs. Sal	479	162	317
Reinstatement	Low (Resilient) vs. Sal	358	136	222
	High (Vulnerable) vs. Sal	301	155	146

A

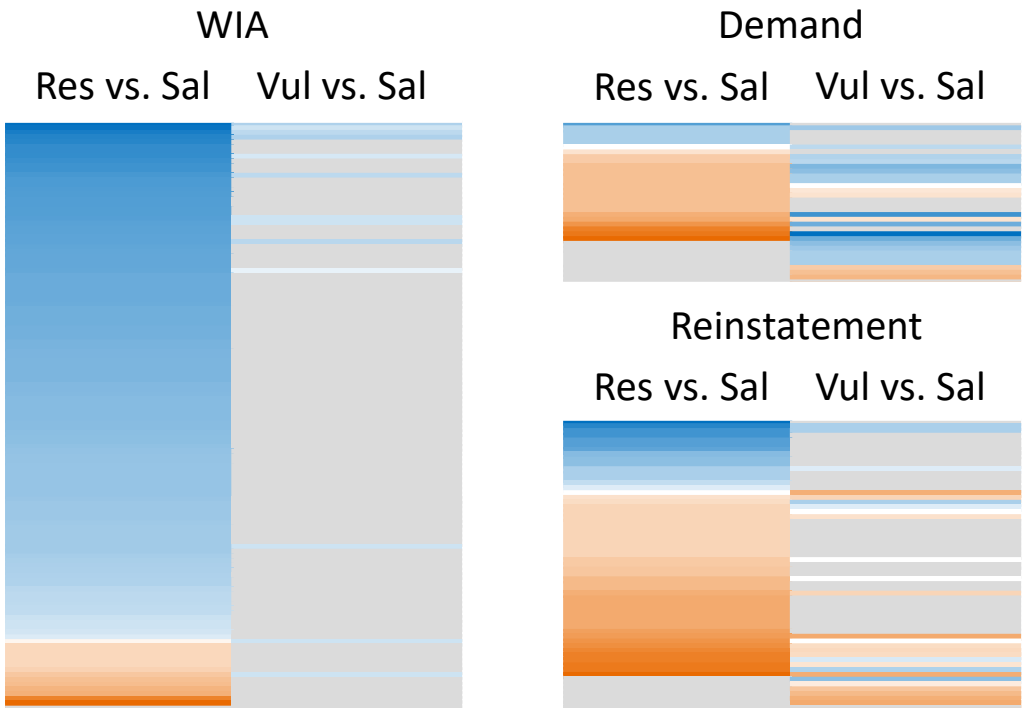

B

Paradigm	Group	# Sig. Pathways
WIA	High (Resilient) vs. Sal	111
	Low (Vulnerable) vs. Sal	5
Demand	High α (Resilient) vs. Sal	15
	Low α (Vulnerable) vs. Sal	14
Reinstatement	Low (Resilient) vs. Sal	49
	High (Vulnerable) vs. Sal	8

A

Module	# of Genes	MeDC	p-value
"darkturquoise"	160	-7.41	<2.20E-16
"plum1"	86	-1.40	<2.20E-16
"purple"	531	0.43	<2.20E-16
"saddlebrown"	125	-0.38	0.02
"steelblue"	124	-2.85	0.02

B

Gene Ontology Term	# of Genes	Fold Enrichment	q-value
Biological process			
CNS myelination	7	62.66	2.64E-07
Oligodendrocyte development	9	36.62	4.11E-08
Oligodendrocyte differentiation	11	23.22	7.01E-08
Axon ensheathment	11	21.98	4.06E-08
Gliogenesis	12	9.07	1.97E-05
Cellular component			
Myelin sheath	8	33.15	6.12E-07

C

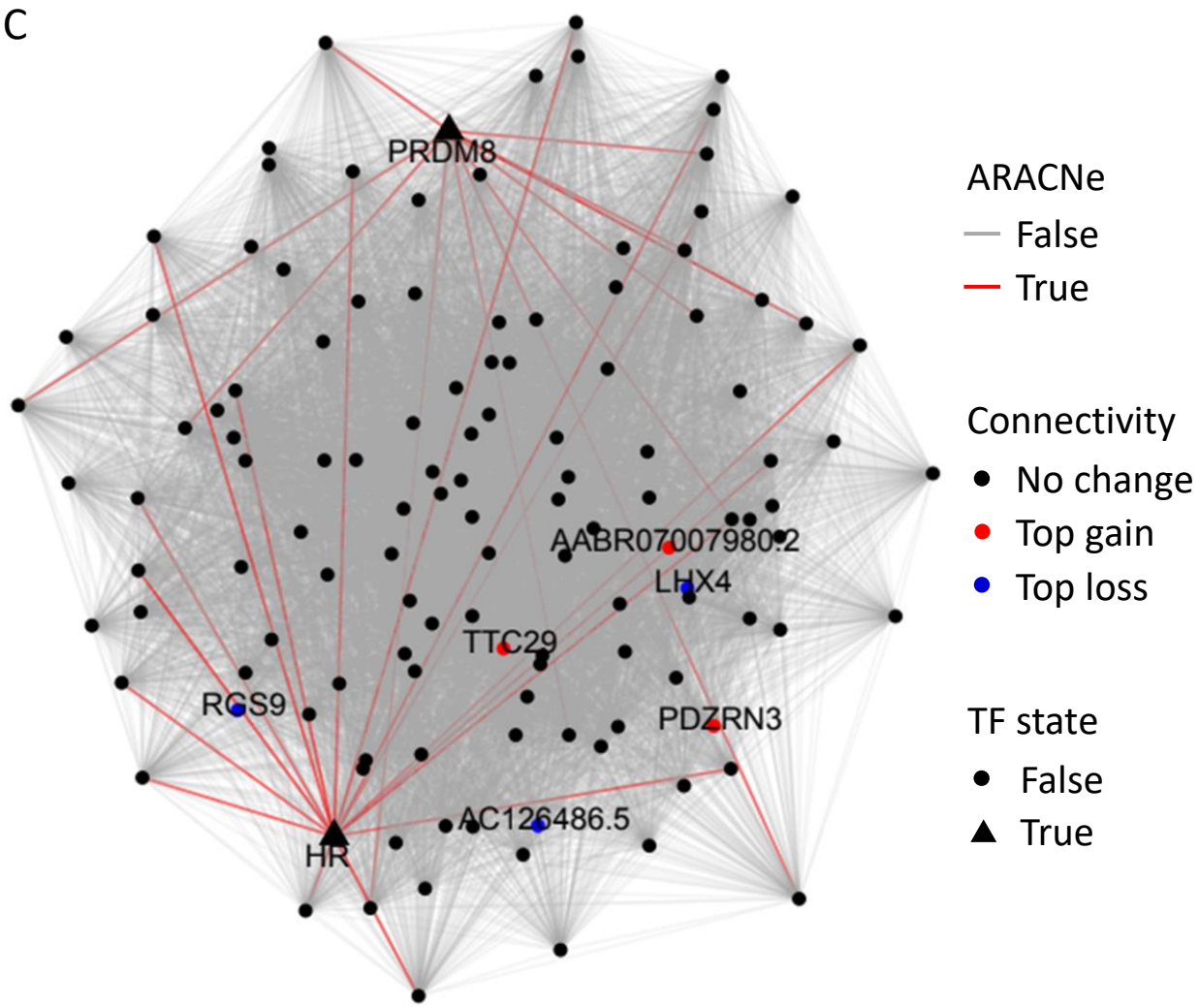

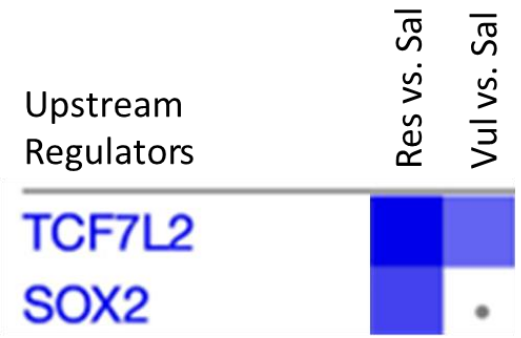
Upstream Regulators
Res vs. Sal
Vul vs. Sal
TCF7L2
SOX2

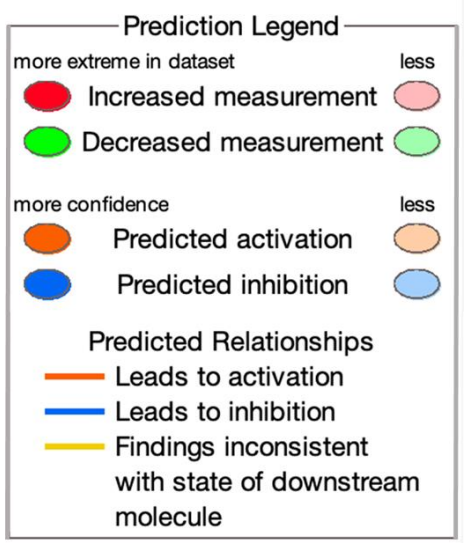
Prediction Legend
more extreme in dataset
less
Increased measurement
Decreased measurement
more confidence
less
Predicted activation
Predicted inhibition
Predicted Relationships
Leads to activation
Leads to inhibition
Findings inconsistent with state of downstream molecule

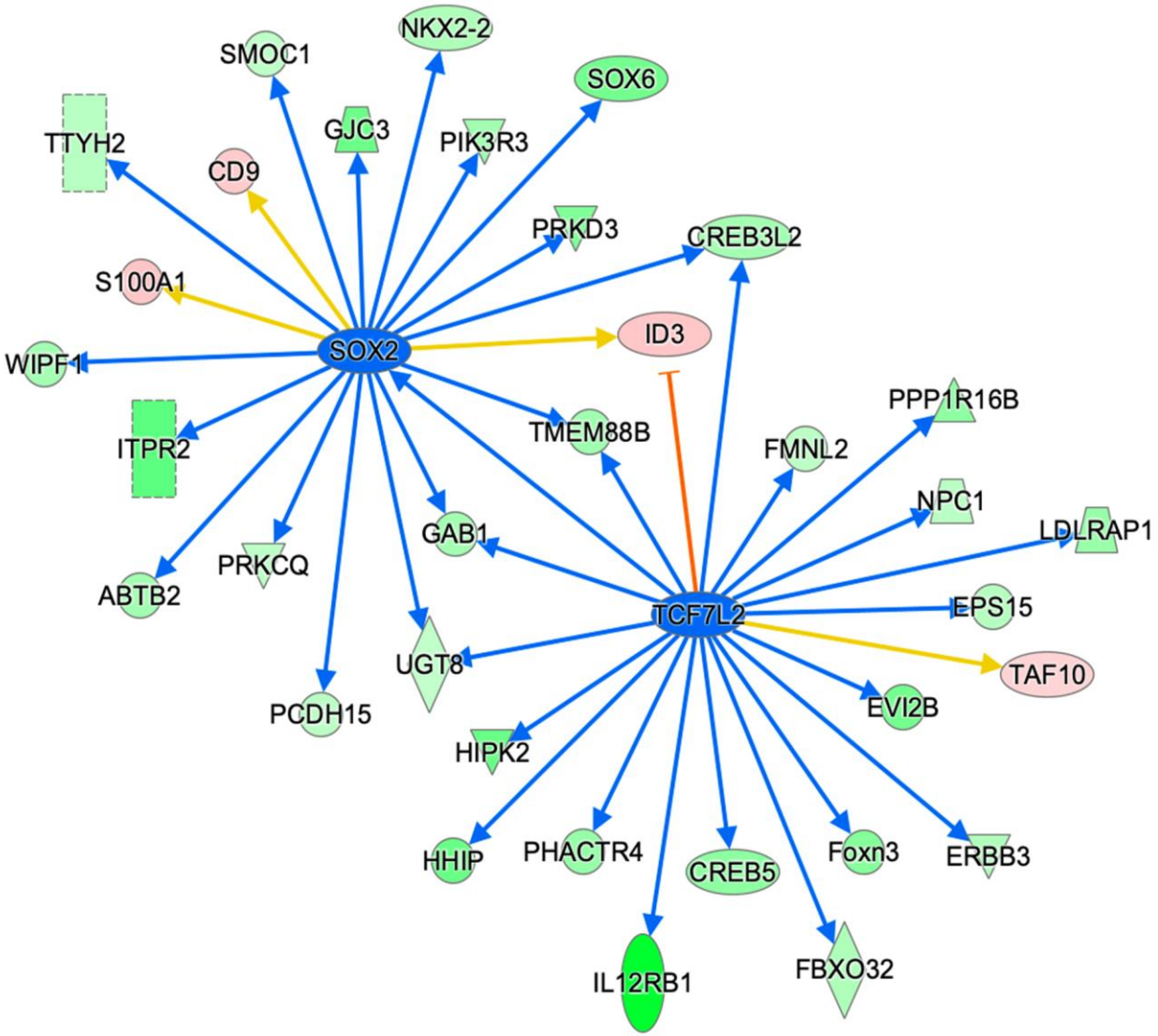
NKX2-2
SMOC1
SOX6
TTYH2
GJC3
PIK3R3
CD9
PRKD3
CREB3L2
S100A1
ID3
SOX2
WIPF1
PPP1R16B
TMEM88B
ITPR2
FMNL2
NPC1
GAB1
LDLRAP1
PRKCQ
ABTB2
TCF7L2
EPS15
UGT8
TAF10
EVI2B
PCDH15
HIPK2
HHIP
PHACTR4
CREB5
Foxn3
ERBB3
IL12RB1
FBXO32

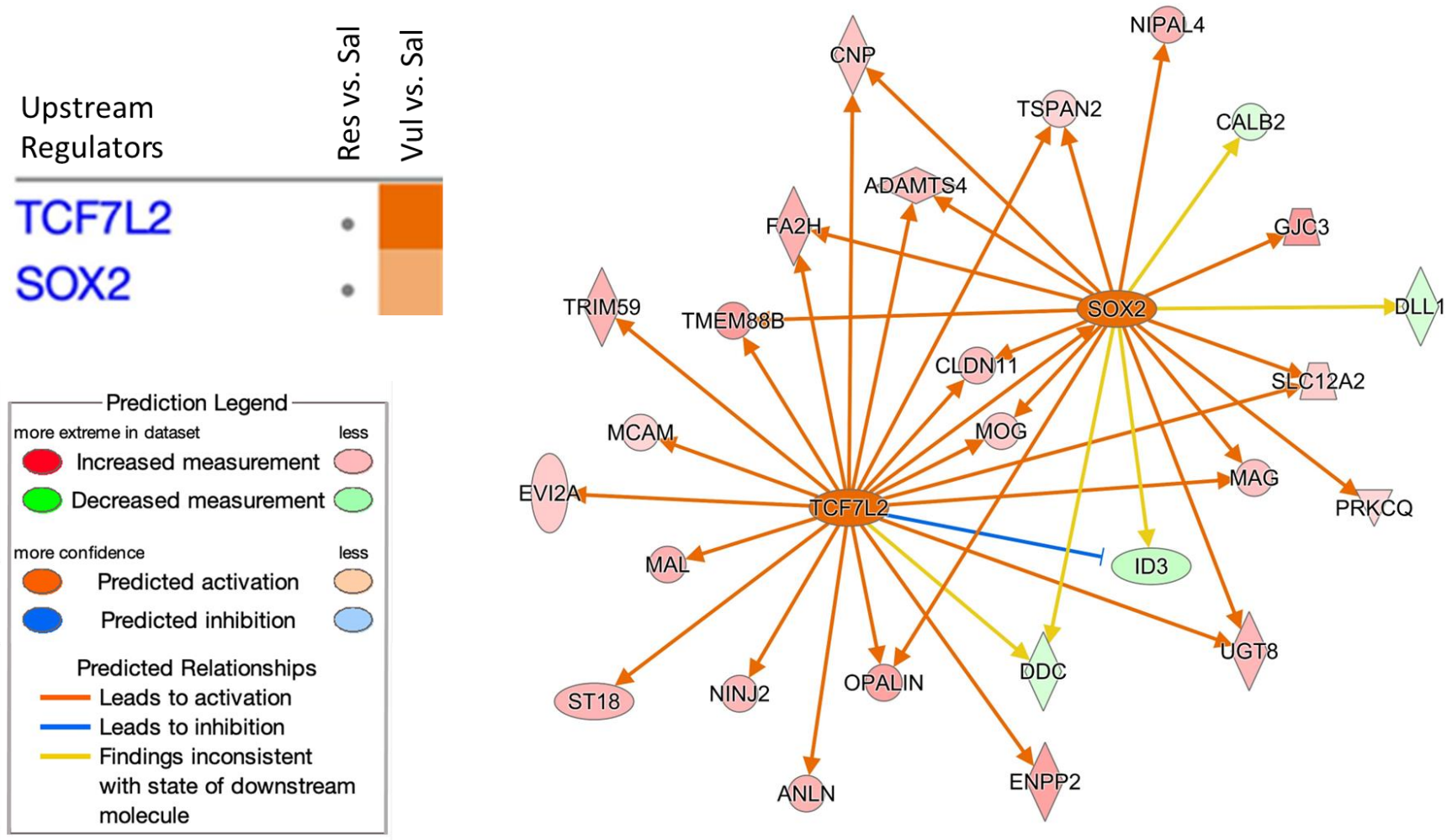
Upstream Regulators
Res vs. Sal
Vul vs. Sal
TCF7L2
SOX2
Prediction Legend
more extreme in dataset
less
Increased measurement
Decreased measurement
more confidence
less
Predicted activation
Predicted inhibition
Predicted Relationships
Leads to activation
Leads to inhibition
Findings inconsistent with state of downstream molecule
NIPAL4
CNP
TSPAN2
CALB2
ADAMTS4
FA2H
GJC3
TRIM59
TMEM88B
SOX2
DLL1
CLDN11
SLC12A2
MCAM
MOG
MAG
EVI2A
TCF7L2
PRKCQ
MAL
ID3
UGT8
DDC
ST18
NINJ2
OPALIN
ANLN
ENPP2

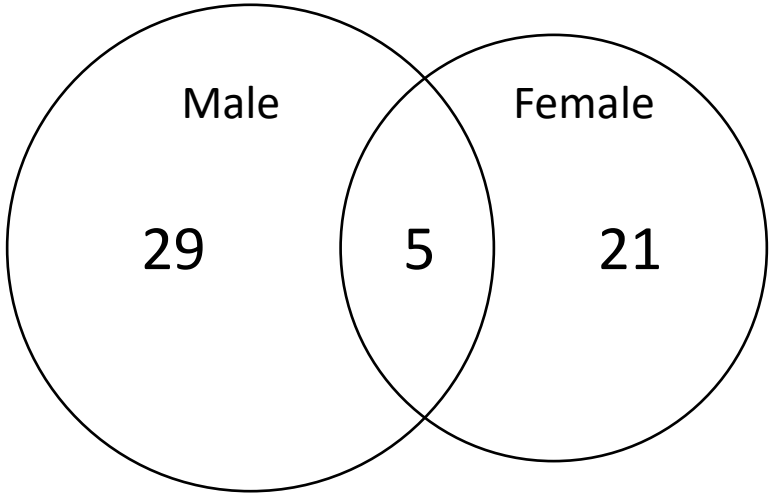
Male
Female
29
5
21

A

Module	# of Genes	MeDC	p-value
"blue"	4218	-0.04	0.02
"lightcyan"	349	-0.41	<2.20E-16
"magenta"	987	-0.14	0.04
"darkorange"	162	-0.59	<2.20E-16
"skyblue"	154	-4.56	<2.20E-16
"white"	158	-3.81	<2.20E-16

B

Gene Ontology Term	# of Genes	Fold Enrichment	q-value
Biological process			
Immunoglobulin mediated immune response	9	9.86	7.98E-03
B cell mediated immunity	9	9.48	5.45E-03
Lymphocyte mediated immunity	9	7.11	2.63E-02
Leukocyte mediated immunity	10	6.38	2.67E-02

A

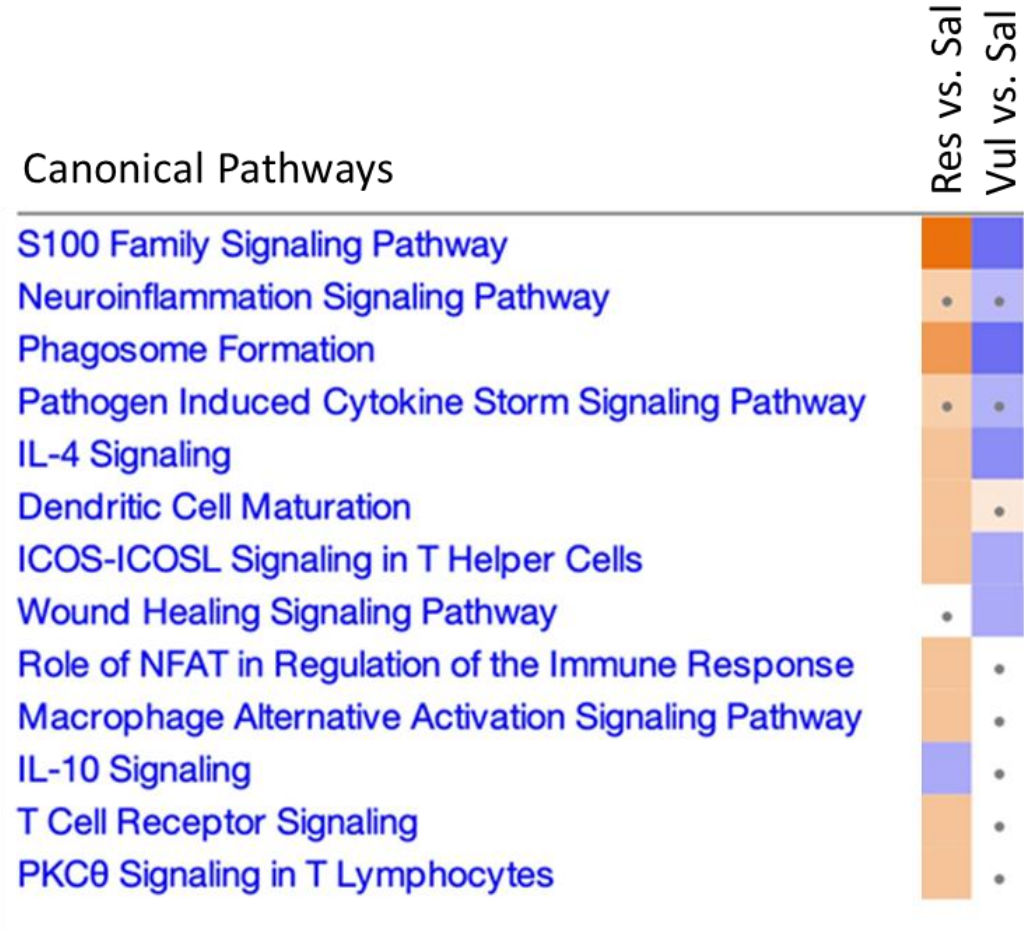
Canonical Pathways
Res vs. Sal
Vul vs. Sal
S100 Family Signaling Pathway
Neuroinflammation Signaling Pathway
Phagosome Formation
Pathogen Induced Cytokine Storm Signaling Pathway
IL-4 Signaling
Dendritic Cell Maturation
ICOS-ICOSL Signaling in T Helper Cells
Wound Healing Signaling Pathway
Role of NFAT in Regulation of the Immune Response
Macrophage Alternative Activation Signaling Pathway
IL-10 Signaling
T Cell Receptor Signaling
PKCθ Signaling in T Lymphocytes

B

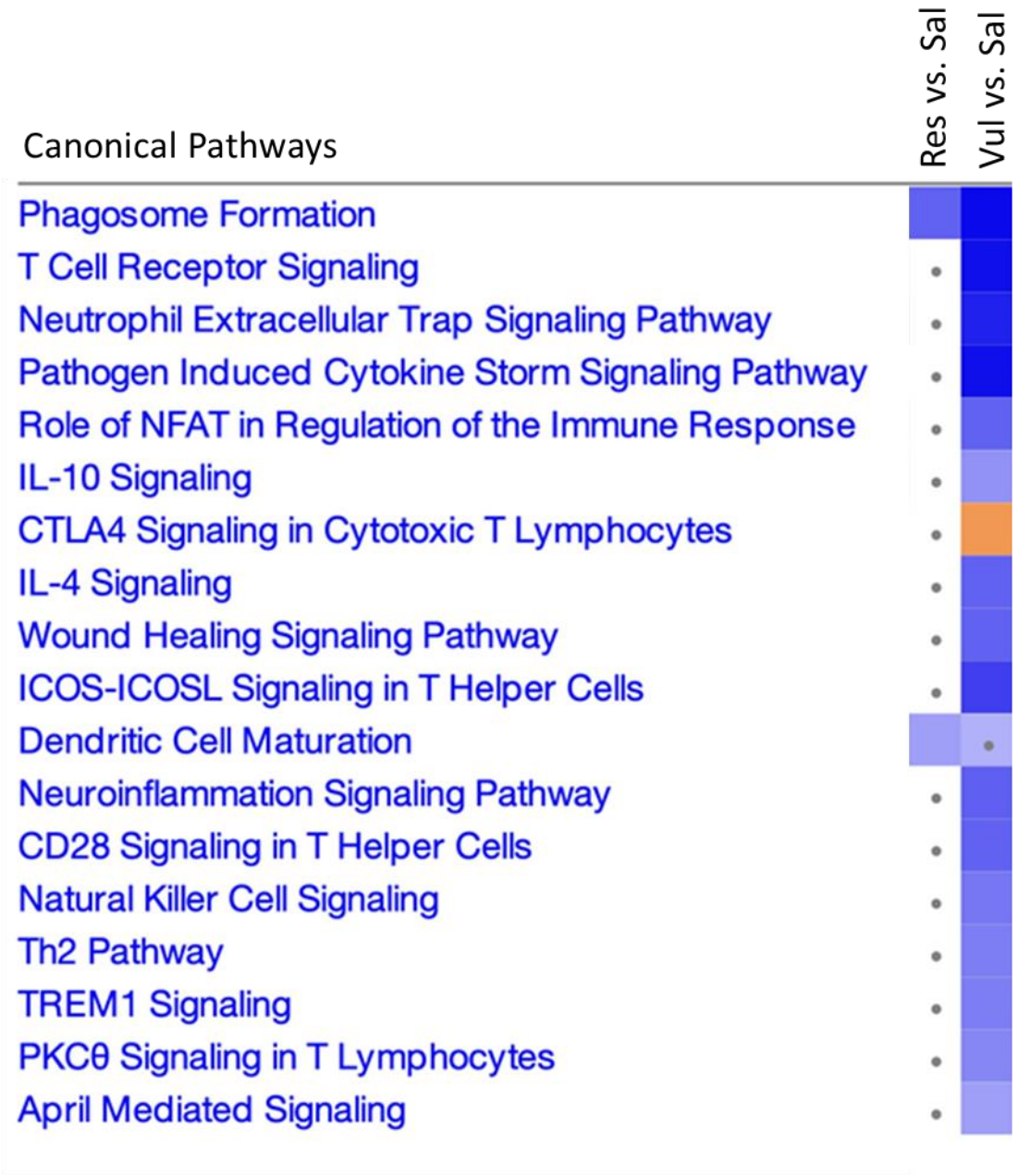
Canonical Pathways
Res vs. Sal
Vul vs. Sal
Phagosome Formation
T Cell Receptor Signaling
Neutrophil Extracellular Trap Signaling Pathway
Pathogen Induced Cytokine Storm Signaling Pathway
Role of NFAT in Regulation of the Immune Response
IL-10 Signaling
CTLA4 Signaling in Cytotoxic T Lymphocytes
IL-4 Signaling
Wound Healing Signaling Pathway
ICOS-ICOSL Signaling in T Helper Cells
Dendritic Cell Maturation
Neuroinflammation Signaling Pathway
CD28 Signaling in T Helper Cells
Natural Killer Cell Signaling
Th2 Pathway
TREM1 Signaling
PKCθ Signaling in T Lymphocytes
April Mediated Signaling

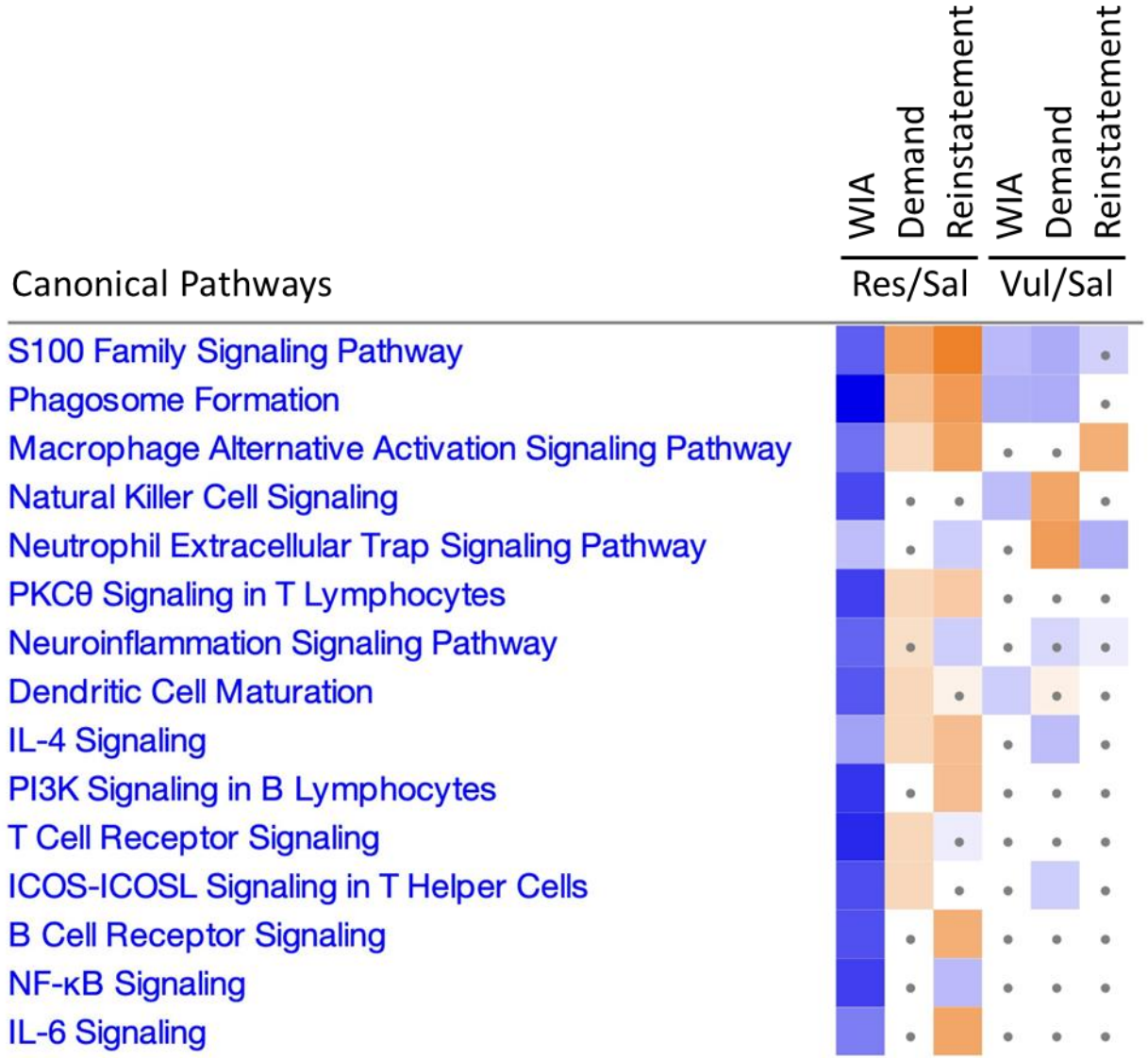
Canonical Pathways
WIA
Demand
Reinstatement
WIA
Demand
Reinstatement
Res/Sal
Vul/Sal
S100 Family Signaling Pathway
Phagosome Formation
Macrophage Alternative Activation Signaling Pathway
Natural Killer Cell Signaling
Neutrophil Extracellular Trap Signaling Pathway
PKCθ Signaling in T Lymphocytes
Neuroinflammation Signaling Pathway
Dendritic Cell Maturation
IL-4 Signaling
PI3K Signaling in B Lymphocytes
T Cell Receptor Signaling
ICOS-ICOSL Signaling in T Helper Cells
B Cell Receptor Signaling
NF-κB Signaling
IL-6 Signaling

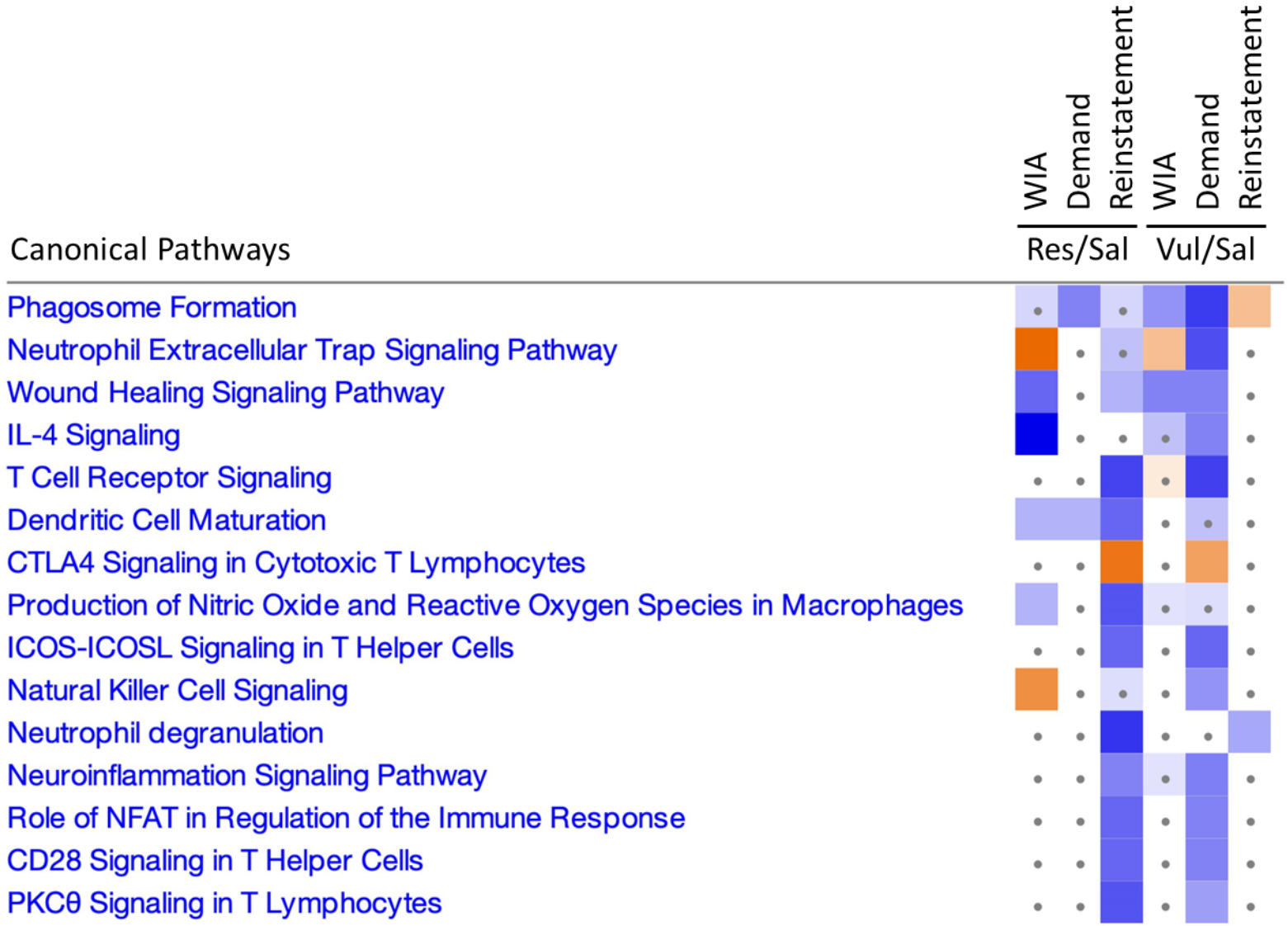
Canonical Pathways
WIA
Demand
Reinstatement
WIA
Demand
Reinstatement
Res/Sal
Vul/Sal
Phagosome Formation
Neutrophil Extracellular Trap Signaling Pathway
Wound Healing Signaling Pathway
IL-4 Signaling
T Cell Receptor Signaling
Dendritic Cell Maturation
CTLA4 Signaling in Cytotoxic T Lymphocytes
Production of Nitric Oxide and Reactive Oxygen Species in Macrophages
ICOS-ICOSL Signaling in T Helper Cells
Natural Killer Cell Signaling
Neutrophil degranulation
Neuroinflammation Signaling Pathway
Role of NFAT in Regulation of the Immune Response
CD28 Signaling in T Helper Cells
PKCθ Signaling in T Lymphocytes

A

Module	# of Genes	MeDC	p-value
"brown4"	159	-2.61	<2.20E-16
"darkgreen"	292	-0.08	0.02
"brown"	2064	0.05	<2.20E-16
"royalblue"	302	-0.05	<2.20E-16
"grey60"	369	-0.04	0.02
"mediumpurple3"	177	-5.36	<2.20E-16

B

Gene Ontology Term	# of Genes	Fold Enrichment	q-value
Biological process			
Negative regulation of phosphate metabolic process	15	3.62	1.56E-02
Negative regulation of protein metabolic process	27	2.92	1.41E-03
Negative regulation of nitrogen compound metabolic process	44	2.12	2.75E-03
metabolic process	99	1.42	4.54E-02

Motif Logo	Name	Comparison	q-value		
			WIA	Demand	Reinstatement
	Fos (AP1)	Mor vs. Sal	<0.0001	<0.0001	<0.0001
		Res vs. Vul	-	-	-
	Mef2d	Mor vs. Sal	0.0001	<0.0001	-
		Res vs. Vul	-	<0.0001	0.0412
	Atoh1 (bHLH)	Mor vs. Sal	-	<0.0001	-
		Res vs. Vul	-	<0.0001	-
	Npas4 (bHLH)	Mor vs. Sal	-	<0.0001	<0.0001
		Res vs. Vul	-	-	0.0028
	Pgr (NR)	Mor vs. Sal	-	-	<0.0001
		Res vs. Vul	-	-	-